InISAR Imaging of Dechirp Data under Squint Model

Biao Tian, Gang Li, Shiyou Xu, and Zengping Chen
Science and Technology on Automatic Target Recognition Laboratory
National University of Defense Technology, Changsha, China

Abstract— Aiming at InISAR imaging of dechirp data under squint modela new method based on squint iteration optimization (SIO) and distortion correction (DC) is proposed in this paper. The squint model induces the influence of accessional phase and image distortion. The 3D imaging results degrade seriously when the squint angle is big. Through a few times of squint iteration optimization and distortion correction, the estimation precision and the imaging quality are improved. Simulation results demonstrate the effectiveness of the method.

1. INTRODUCTION

Inverse synthetic aperture radar (ISAR) [1, 2] can generate 2D high resolution images of non-cooperative targets from a long distance and is widely used for military and civilian purposes. The ISAR image, however, is just the Range-Doppler plane projection of a three spatial dimensional target which results in the loss of structure information. In order to enhance the target recognition probability, the interferometric ISAR (InISAR) [3–5] technique is presented to achieve the third dimension of the target. In traditional InISAR imaging systems, three receiving antennas are mostly used [3, 4]. Using the phase difference of the three 2D complex ISAR images, the corresponding position of each scattering can be achieved.

As is known to all, the ISAR image plane is related to the targets motion with respect to the radar line of sight (LOS). For convenience, the target is generally assumed to be located close to the antenna axis in traditional InISAR imaging systems, which is called the normal mode. In practice, however, the target is usually far away from the antenna axis [6–8], which is called the squint mode. A novel InISAR imaging algorithm based on dominant scatterers is proposed in literature [6]. The phase ambiguity induced by squint is inevitable since the same reference range is used in stretch processing. Moreover, the difference of system structure limits the application of image registration using parameter estimation of targets angular motion. In literature [7], the approximation introduced to deal with the coupling of squint additive phase and target coordinates degrades the image quality. Literature [8] combines the nonlinear least square (NLS) and coordinates transform (CT) to estimate the target coordinates. The computation efficiency is decreased since NLS is applied.

Aiming at above problems we propose a new squint model InISAR imaging method based on squint iteration optimization. The remainder of this paper is organized as follows. In Section 2, the InISAR imaging geometry and signal model is described. Section 3 analyzes the influence of squint model. The new squint model InISAR imaging method based on squint iteration optimization is detailed in Section 4. Simulation results and performance analysis are reported in Section 5, followed by conclusion in Section 6.

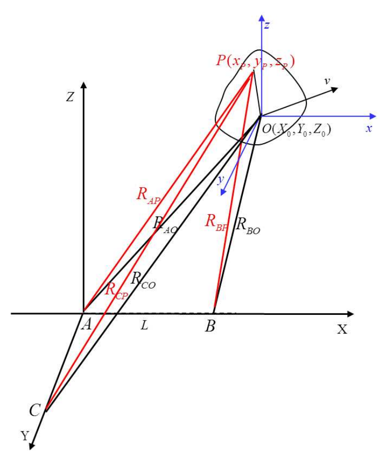

Figure 1: Three-receiver InISAR imaging geometry.

2. SIGNAL MODEL OF DECHIRP DATA FOR INISAR SYSTEM

The geometry of three-receiver InISAR imaging system is shown in Figure 1. In the system, A is the transmitter and receiver while B and C only receive signal. The initial location of the target center is (X_0, Y_0, Z_0) in the XYZ coordinate system. The initial distance from the antenna A can be denoted as $R_0 = \sqrt{X_0^2 + Y_0^2 + Z_0^2}$. The ISAR image of each antenna can be written as [8]:

$$S_A(f, f_m) = A_P T_P T_1 \text{sinc}\left[T_P\left(f + \frac{2\gamma}{c} R_{\Delta AP0}\right)\right] \text{sinc}\left[T_1\left(f_m + \frac{2V_{AP}}{\lambda}\right)\right] \exp\left\{-j\frac{4\pi}{\lambda} R_{\Delta AP0}\right\} \quad (1)$$

$$\begin{aligned} S_B(f, f_m) = {} & A_P T_P T_1 sinc\left[T_P\left(f + \frac{\gamma}{c}\left(R_{\Delta AP0} + R_{\Delta BP0}\right)\right)\right] \\ & \text{sinc}\left[T_1\left(f_m + \frac{V_{AP} + V_{BP}}{\lambda}\right)\right] \exp\left\{-j\frac{2\pi}{\lambda}\left(R_{\Delta AP0} + R_{\Delta BP0}\right)\right\} \end{aligned} \quad (2)$$

$$\begin{aligned} S_C(f, f_m) = {} & A_P T_P T_1 \text{sinc}\left[T_P\left(f + \frac{\gamma}{c}\left(R_{\Delta AP0} + R_{\Delta CP0}\right)\right)\right] \\ & \text{sinc}\left[T_1\left(f_m + \frac{V_{AP} + V_{CP}}{\lambda}\right)\right] \exp\left\{-j\frac{2\pi}{\lambda}\left(R_{\Delta AP0} + R_{\Delta CP0}\right)\right\} \end{aligned} \quad (3)$$

where A_P is the scattering amplitude, T_P is the pulse width, T_1 is the imaging time, $R_{\Delta AP} = R_{AP} - R_{refA}$, R_{AP} is the distance between scattering point P and antenna A, R_{refA} is the reference range, V_{AP} is the variety rate. The interferometric phase could be expressed as follows

$$\Delta\varphi_{AB} = Angle\left(S_B(f, f_m) S_A^*(f, f_m)\right) = \frac{2\pi}{\lambda}(R_{\Delta AP0} - R_{\Delta BP0}) \triangleq \frac{2\pi}{\lambda}\Delta R_{AB0} \quad (4)$$

$$\Delta\varphi_{AC} = Angle\left(S_C(f, f_m) S_A^*(f, f_m)\right) = \frac{2\pi}{\lambda}(R_{\Delta AP0} - R_{\Delta CP0}) \triangleq \frac{2\pi}{\lambda}\Delta R_{AC0} \quad (5)$$

For normal model, the same reference ranges are chosen to carry out dechirp processing for each antenna, i.e. $R_{refA} = R_{refB} = R_{refC} = R_{AO}$, then

$$\Delta R_{AB} = (R_{AP} - R_{AO}) - (R_{BP} - R_{AO}) \approx \frac{Lx_P}{R_0} \quad (6)$$

$$\Delta R_{AC} = (R_{AP} - R_{AO}) - (R_{CP} - R_{AO}) \approx \frac{Ly_P}{R_0} \quad (7)$$

From the above four formularies, we have

$$x_P = \frac{\lambda R_0 \Delta\varphi_{AB}}{2\pi L} \quad (8)$$

$$y_P = \frac{\lambda R_0 \Delta\varphi_{AC}}{2\pi L} \quad (9)$$

Meanwhile, the Z coordinate can be obtained by scaling of the ISAR image. In this way, the three dimensions of the target are achieved.

3. INFLUENCE OF SQUINT MODEL

3.1. Accessional Interferometric Phase

The interferometric phase of point P can be rewritten as

$$\Delta\varphi_{AB} = \frac{2\pi}{\lambda}(R_{\Delta AP0} - R_{\Delta BP0}) = \frac{2\pi}{\lambda}\left(\frac{2Lx_P}{R_{AP0} + R_{BP0}} + \frac{2LX_0 - L^2}{R_{AP0} + R_{BP0}} - \frac{2LX_0 - L^2}{R_{AO0} + R_{BO0}}\right) \quad (10)$$

Let $\varphi_1 = \frac{2\pi}{\lambda} \cdot \frac{2Lx_P}{R_{AP0} + R_{BP0}}$, $\varphi_2 = \frac{2\pi}{\lambda} \cdot \frac{2LX_0 - L^2}{R_{AP0} + R_{BP0}}$, $\varphi_3 = -\frac{2\pi}{\lambda} \cdot \frac{2LX_0 - L^2}{R_{AO0} + R_{BO0}}$, where φ_1 is the main interferometric phase that contains the coordinate information while φ_2 and φ_3 are the accessional phases caused by squint view of the X direction. We call them as main phase and accessional phase respectively. Then $\Delta\varphi_{AB} = \varphi_1 + \varphi_2 + \varphi_3$.

When the radar works at the normal model, namely $\varphi_2+\varphi_3=0$, the coordinate x_P of the point P can be simplified as Eq. (8). When the radar works at squint model, however, the interferometric phase becomes ambiguous if $\varphi_2+\varphi_3$ is big enough. Moreover, the accessional phases are not the same to all points, since they are correlative with the point location too. Only after they are compensated, can we achieve accurate 3D InISAR image.

3.2. Image Distortion

The down-range coordinates R of 2D ISAR image is not directly in accordance with the z-axis coordinate of the target when the squint angle is too big. Through the CT method, the true coordinates of the target (x, y, z) can be obtained from the distorted coordinates (x, y, r).

The projection coordinate of P at R-axis of the radar LOS coordinate is

$$r = x\cos\varphi\cos\theta + y\cos\varphi\sin\theta + z\sin\varphi \tag{11}$$

where θ and φ are the azimuth and pitching angle of the LOS direction. As we can see, the obtained down-range coordinate is related to each of the three coordinates of point P, which results in distortion of the final 3D InISAR image.

4. INISAR IMAGING BASED ON SQUINT ITERATION OPTIMIZATION

As analyzed in Section 3.2, only after the compensation of the accessional phases is carried out, can high quality 3D InISAR results be achieved. In this section, we propose a method named squint iteration optimization to carry out high precision interferometric processing. From Eq. (10), we can get the true x-coordinate and y-coordinate of scattering point as

$$x_P = \frac{R_{AP0}+R_{BP0}}{2L}\cdot\left(\frac{\lambda}{2\pi}\Delta\varphi_{AB} - \frac{2LX_0-L^2}{R_{AP0}+R_{BP0}} + \frac{2LX_0-L^2}{R_{AO0}+R_{BO0}}\right) \tag{12}$$

$$y_P = \frac{R_{AP0}+R_{CP0}}{2L}\cdot\left(\frac{\lambda}{2\pi}\Delta\varphi_{AC} - \frac{2LX_0-L^2}{R_{AP0}+R_{CP0}} + \frac{2LX_0-L^2}{R_{AO0}+R_{CO0}}\right) \tag{13}$$

As can be seen from the above two equations, the true location of scattering point is related to R_{AP0}, R_{BP0} and R_{CP0}, and, which are also associated with x_P, y_P and z_P. In order to achieve accurate interferometric result, a few iterations should be carried out to achieve improvement. The initial value of the iteration can be used as that in Eqs. (8) and (9). Then we can calculate the distance value of the scattering point to each antenna

$$R_{AP0} = \sqrt{(X_0+x_P)^2+(Y_0+y_P)^2+(Z_0+z_P)^2} \tag{14}$$

$$R_{BP0} = \sqrt{(X_0+x_P-L)^2+(Y_0+y_P)^2+(Z_0+z_P)^2} \tag{15}$$

$$R_{CP0} = \sqrt{(X_0+x_P)^2+(Y_0+y_P-L)^2+(Z_0+z_P)^2} \tag{16}$$

After this step, the iteration can be carried out and updated.

The image distortion correction could be achieved using the following inverse CT:

$$z_P = (r - x\cos\varphi\cos\theta + y\cos\varphi\sin\theta)/\sin\varphi \tag{17}$$

As we can see, the true z-coordinate meets the equation. To obtain 3D InISAR image more precisely, the distortion correction and squint iteration improvement should be carried out in the same step. The times of iterations should be decided by convergence condition of practical requirement.

The steps of squint iteration optimization and distortion correction can be summarized as:

1) Calculate the interferometric phase $\Delta\varphi_{AB}$ and $\Delta\varphi_{AC}$ using Eqs. (4) and (5).
2) Obtain the initial coordinate x_P and y_P using Eqs. (8) and (9), while $z_P = r$ by scaling of ISAR image.
3) Get the distance values of each scattering point to each antenna using Eqs. (14)–(16).
4) Update the coordinate x_P and y_P using Eqs. (12) and (13).
5) Update the coordinate z_P using Eq. (17).
6) Repeat steps 3–5 until the convergence condition is achieved.

Using the method, all the 3D spatial coordinates of each scattering point on the target are obtained, and the high precision 3D InISAR image is obtained.

5. SIMULATION RESULTS AND ANALYSIS

In order to test the analysis and 3D InISAR imaging algorithm under squint model, the simulation of a target with stable motion in the far-field is carried out. The parameters of the radar system are as follows. The carrier frequency is 10 GHz, the bandwidth is 500 MHz, the PRF is 200 Hz, the pulse width is 50 µs, the pulses used for imaging is 256. The locations of antenna A/B/C are (0, 0, 0)/(100 m, 0, 0)/(0, 100 m, 0). The target contains 6 scattering points, whose three dimensional positions are (7, 5, 5), (−5, 5, 15), (3, 15, 5), (−1, 15, 15), (0, 2, 9), (7, 1 0, 10). The velocity of it is (1000, 5000, 1000) m/s. In the following simulations, three different instances are set. We call them normal model in which the targets initial location is (50 m, 50 m, 1000 km), and small squint model in which the targets initial location is (20 km, 20 km, 1000 km), and squint model in which the targets initial location is (200 km, 250 km, 1000 km).

Firstly, we demonstrate the influence of squint model to the interferometric phase. According

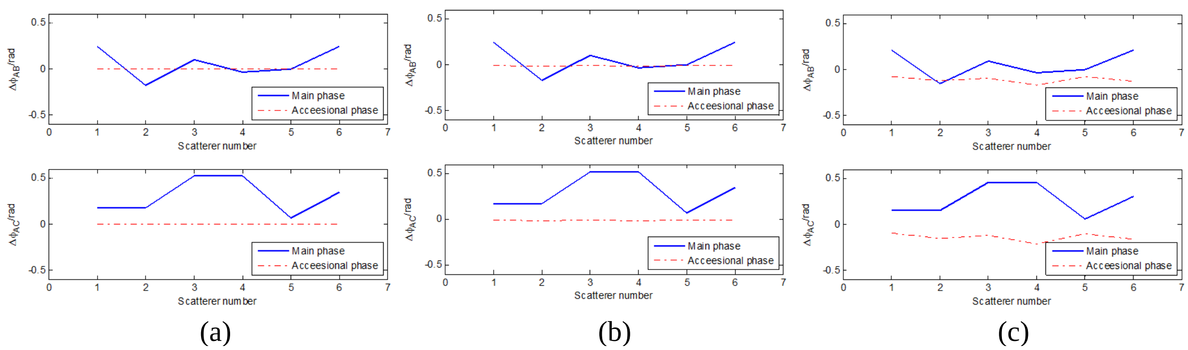

Figure 2: Comparison of main phase and accessional phase. (a) Normal model. (b) Small squint model. (c) Squint model.

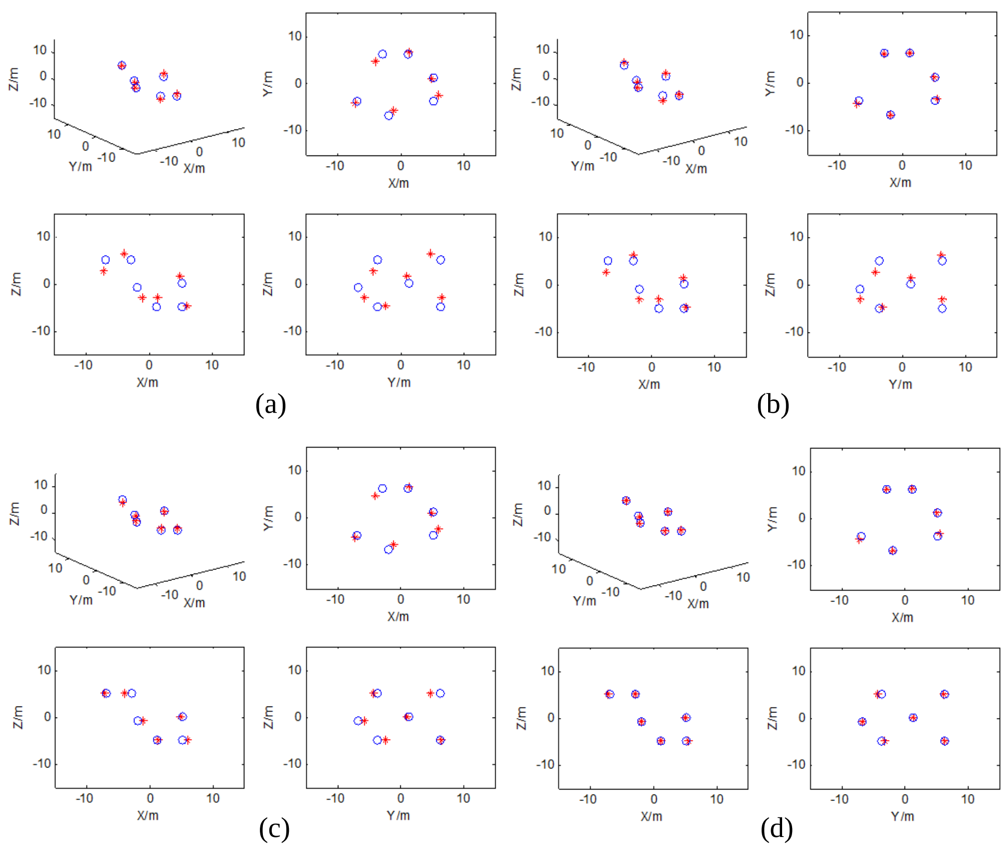

Figure 3: 3D imaging result under squint model. (a) Traditional method. (b) SIO only. (c) DC only. (d) Combination of SIO and DC.

to the analysis in Eq. (10), the main phase and accessional phase will be compared.

As Figure 2 shows, the accessional phase $\varphi_2 + \varphi_3$ is nearly zero, and it could be neglected in normal model. It increases with the increment of squint angle. The accessional phase turns comparable large as the main phase (Figure 2(c)), so we should not neglect the influence of squint model any more. Once the coordinates are simply obtained by using Eqs. (8) and (9), the 3D InISAR imaging results are in bad quality.

Then, we demonstrate the effectiveness of InISAR imaging based on squint iteration optimization and distortion correction method for squint mode. Figure 3 shows the InISAR imaging results using different methods, in which the actual scatterer distribution and the imaging results are represented by $\circ$ and $*$, respectively. As we can see from Figures 3(a) and (b), the estimated coordinates x and y after squint iteration optimization are basically equal to the actual target model. The z coordinate, however, still departs from the target model due to the squint degree. By comparison of Figures 3(a) and (c), we can see that the z coordinates are approximately equal to the set ones after distortion correction. Figure 3(d) shows the 3D imaging results using the combination of squint iteration improvement and distortion correction. The z-coordinate is consistent with that of the target model as well. In a word, the estimated 3D coordinates based on the proposed method highly matches the actual target model.

6. CONCLUSION

For the application of InISAR, the target location usually departs from the perpendicular bisector of the baseline. The paper proposes a new 3D InISAR imaging algorithm under squint model by squint iteration optimization and distortion correction, the 3D reconstruction performance and quality are improved. Simulation results demonstrate that the algorithm is effective, achieving high quality 3D InISAR images consequently.

ACKNOWLEDGMENT

This work was supported by Hunan province innovation foundation for postgraduate (CX2014B020), and National University of Defense Technology innovation foundation for excellent postgraduate (B140405).

REFERENCES

1. Chen, C. C. and H. C. Andrews, "Target-motion-induced radar imaging," *IEEE Trans. on Aerosp. Electron. Syst.*, Vol. 16, No. 1, 2–14, 1980.
2. Delisle, G. Y. and H. Wu, "Moving target imaging and trajectory computation using ISAR," *IEEE Trans. on Aerosp. Electron. Syst.*, Vol. 30, No. 3, 887–899, 1994.
3. Zhang, Q., T. S. Yeo, G. Du, and S. Zhang, "Estimation of three-dimensional motion parameters in interferometric ISAR imaging," *IEEE Trans. Geosci. Remot Sen.*, Vol. 42, No. 2, 292–300, 2004.
4. Wang, G. Y., X. Xia, and V. C. Chen, "Three-dimensional ISAR imaging of maneuvering targets using three receivers," *IEEE Trans. Image Proc.*, Vol. 10, No. 3, 436–447, 2001.
5. Felguera-Martin, D., J. T. Gonzalez-Partida, and M. Burgos-Garcia, "Interferometric ISAR imaging on martime target applications: Simulation of realistic targets and dynamics," *Progress In Electromagnetics Research*, Vol. 132, 571–586, 2012.
6. Li, L. Y., H. W. Liu, B. Jiu, et al., "An interferometric inverse synthetic aperture radar imaging algorithms for squint model," *J. Xi'an Jiao Tong University*, Vol. 42, No. 10, 1290–1294, 2008.
7. Ma, C. Z., T. S. Yeo, H. S. Tan, et al., "Interferometric ISAR imaging on squint model," *Progress In Electromagnetics Research L*, Vol. 2, 125–133, 2008.
8. Liu, C. L., F. He, X. Z. Gao, et al., "Squint-mode InISAR imaging based on nonlinear least square and coordinates transform," *Sci China Tech. Sci.*, Vol. 54, No. 12, 3332–3340, 2011.